Spin-Orbit Coupling and Electron Spin Resonance Theory for Carbon Nanotubes

A. De Martino,[1] R. Egger,[1] K. Hallberg,[2] and C. A. Balseiro[2]
[1]*Institut für Theoretische Physik, Heinrich-Heine Universität, D-40225 Düsseldorf, Germany*
[2]*Instituto Balseiro, Centro Atomico, 8400 S.C. de Bariloche, Argentina*
(Received 9 October 2001; published 3 May 2002)

A theoretical description of electron spin resonance (ESR) in 1D interacting metals is given, with primary emphasis on carbon nanotubes. The spin-orbit coupling is derived, and the resulting ESR spectrum is analyzed using a low-energy field theory. Drastic differences in the ESR spectra of single-wall and multiwall nanotubes are found. For single-wall tubes, the predicted double peak spectrum is linked to spin-charge separation. For multiwall tubes, a single narrow asymmetric peak is expected.

DOI: 10.1103/PhysRevLett.88.206402 PACS numbers: 71.10.–w, 73.63.Fg, 76.30.–v

Electron spin resonance (ESR) serves as a valuable tool to experimentally probe the intrinsic spin dynamics of many systems. In ESR experiments, one applies a static magnetic field and measures the absorption of radiation polarized perpendicular to the field direction. In the absence of SU(2) spin symmetry breaking terms in the system Hamiltonian, the absorption intensity is then simply a δ peak at the Zeeman energy [1]. Since spin-orbit (SO) interactions are generally the leading terms breaking the SU(2) invariance, deviations in the ESR intensity from the δ peak, e.g., shifts or broadenings, are directly connected to these couplings. In this Letter we theoretically address the spin-orbit interaction and the resulting ESR spectrum for interacting 1D metallic conductors, in particular for carbon nanotubes. Nanotubes constitute a new class of mesoscopic quantum wires characterized by the interplay of strong electron-electron interactions, reduced dimensionality, disorder, and unconventional spin dynamics [2–6]. ESR is an important technique to elucidate aspects of this interplay inaccessible to (charge) transport experiments. For interacting many-body systems, surprisingly little is known about ESR although it represents an interesting theoretical problem.

Two main classes of nanotubes may be distinguished, namely, single-wall nanotubes (SWNTs) which consist of just one wrapped-up graphite sheet, and multiwall nanotubes (MWNTs). MWNTs contain additional inner shells, but transport is generally limited to the outermost shell [4]. Evidence for the Luttinger liquid (LL) behavior of interacting 1D electrons has been reported for charge transport in SWNTs [3], where one also expects to find spin-charge separation [5,6]. Conventional wisdom holds that the SO coupling in 1D conductors destroys spin-charge separation [7]. Below we show that this statement is *incorrect*. The SO interaction considered in Ref. [7] was intended for the limited class of semiconductor quantum wires in strong Rashba and confinement electric fields, but in fact does not represent the generic SO Hamiltonian for 1D conductors. The latter is derived below and determines the ESR intensity in SWNTs and MWNTs. A totally different ESR spectrum compared to expectations based on Ref. [7] emerges. In particular, the single δ peak is split into *two* narrow peaks in SWNTs, while for the SO coupling of Ref. [7], the spectrum forms a broad band with thresholds at the lower and upper edges [8]. This qualitative difference can be traced back to the fact that the SO interaction in SWNTs [see Eq. (5) below] does *not* spoil spin-charge separation. Experimental observation of the peak splitting could therefore provide strong evidence for the elusive phenomenon of spin-charge separation. In MWNTs, inner shells cause a rather strong Rashba-type SO coupling, leading instead to a *single* narrow asymmetric ESR peak. To experimentally observe our predictions, it will be crucial to work with samples free of magnetic impurities whose presence has drastically affected previous ESR measurements for nanotubes [4].

In the standard Faraday configuration, the ESR intensity at frequency ω is proportional to the Fourier transform of the transverse spin-spin correlation function [1],

$$I(\omega) = \int dt\, e^{i\omega t} \langle S^+(t) S^-(0) \rangle , \qquad (1)$$

where the static magnetic field points along the z axis and $\vec{S} = \sum_i \vec{S}_i$ is the total spin operator. Equation (1) is connected to the dynamical susceptibility via $I(\omega) \sim \omega \chi''(\omega)$. The Hamiltonian is $H = H_0 + H_Z + H'$, where H_0 represents the SU(2) invariant nanotube Hamiltonian including electron-electron interactions, $H_Z = -BS^z$ is the Zeeman term [9], and H' represents SU(2) breaking terms, in particular the SO coupling. Inserting a complete set of eigenstates $|a\rangle$ of H in Eq. (1), the ESR intensity follows as

$$I(\omega) = \frac{1}{Z} \sum_{a,b} e^{-E_b/T} \delta[\omega - (E_a - E_b)] \, |\langle a|S^-|b\rangle|^2 .$$

If H is SU(2) invariant (apart from H_Z), $I(\omega)$ receives contributions only from matrix elements between eigenstates with equal total spin $S_a = S_b$. Then all states with $S_a^z = S_b^z - 1$ will contribute to form a δ peak at frequency $\omega = B$. At zero temperature, the application of a magnetic field B, taken as large enough to overcome a spin gap possibly present at $B = 0$, leads to a ground state with finite magnetization, $S_0 \neq 0$, and the states with $S_a^z = S_0^z - 1$ yield the δ peak. Any perturbation preserving SU(2) invariance will neither shift nor broaden this peak, even

at finite temperature, and it is therefore crucial to identify H'. For quantum spin chains, staggered magnetic fields and Dzyaloshinskii-Moriya interactions have been emphasized [1].

Let us start with the derivation of the SO interaction in nanotubes. In this derivation we neglect electron-electron interactions which only weakly renormalize the SO strength [10]. In a single-particle picture, the SO interaction then appears because an electron moving in the electrostatic potential $\Phi(\vec{r})$, e.g., due to the ions, sees an effective magnetic field $\vec{v} \times \nabla\Phi$. With $\vec{p} = m\vec{v}$ and the standard Pauli matrices $\vec{\sigma}$, the SO interaction reads in second-quantized form,

$$H' = -\frac{g_e \mu_B}{4m} \int d\vec{r}\, \Psi^\dagger [(\vec{p} \times \nabla\Phi) \cdot \vec{\sigma}] \Psi\,. \quad (2)$$

The electron spinor field $\Psi_\sigma(\vec{r})$, defined on the wrapped graphite sheet, can be expressed in terms of the electron operators c_i for honeycomb lattice site i at $\vec{r}_i$, $\Psi_\sigma(\vec{r}) = \sum_i \chi(\vec{r} - \vec{r}_i) c_{i\sigma}$, where $\chi(\vec{r})$ is the $2p_z$ orbital wave function. The localized orbitals can be chosen as real-valued functions even when hybridization with $2s$ orbitals is taken into account, but their specific form is of no immediate interest here. We then obtain the SO interaction, see also Refs. [11,12],

$$H' = \sum_{\langle jk \rangle} i c_j^\dagger (\vec{u}_{jk} \cdot \vec{\sigma}) c_k + \text{H.c.}\,, \quad (3)$$

which indeed breaks SU(2) symmetry. With obvious modifications, Eq. (3) applies to other 1D conductors and thus represents a generic SO Hamiltonian. The SO vector $\vec{u}_{jk} = -\vec{u}_{kj}$ has real-valued entries,

$$\vec{u}_{jk} = \frac{g_e \mu_B}{4m} \int d\vec{r}\, \Phi(\vec{r}) [\nabla\chi(\vec{r} - \vec{r}_j) \times \nabla\chi(\vec{r} - \vec{r}_k)]\,. \quad (4)$$

The on-site term ($j = k$) is identically zero, and since the overlap decreases exponentially with $|\vec{r}_j - \vec{r}_k|$, we keep only nearest-neighbor terms in Eq. (3). We mention in passing that Eq. (3) has previously been found from the $\vec{k} \cdot \vec{p}$ theory by Ando [12]. However, his approach makes rather special model assumptions and is technically demanding, yet it does not allow us to reliably compute the SO vector $\vec{u}_{jk}$ to better accuracy than specified in Eq. (4). In addition, the effect of SO interactions within the low-energy theory of nanotubes [5] has not been analyzed. We therefore take Eq. (3) as the SO Hamiltonian for SWNTs and MWNTs, with the SO vector (4). This formulation also allows us to incorporate electric fields due to impurities or close-by electrodes in a simple and elegant manner.

Let us first turn to SWNTs, where SO couplings are expected to be small. This can be rationalized from our approach since the SO vector (4) *vanishes* by symmetry for an ideal 2D honeycomb lattice. A finite (nearest-neighbor) SO coupling can only arise due to the curvature of the wrapped sheet, stray fields from nearby gates, or due to defects, all of which break the high symmetry and, in principle, allow for significant SO couplings [6]. Focusing on the curvature-induced SO coupling for nonchiral SWNTs, the SO vector depends only on bond direction, $\vec{u}_{\vec{r}_i, \vec{r}_i + \vec{\delta}_a} = \vec{u}_a$, for the nearest-neighbor bonds $\vec{\delta}_a$ ($a = 1, 2, 3$) of the graphite sheet [2].

To make progress, we employ the effective field theory approach [5]. Neglecting the (here inessential) "flavor" index due to the presence of two Fermi (K) points [2], H_0 then corresponds to a spin-1/2 LL described by charge/spin interaction parameters $K_c < 1, K_s$ and velocities $v_{c/s} = v_F/K_{c/s}$ with the Fermi velocity $v_F = 8 \times 10^5$ m/sec; SU(2) invariance of H_0 fixes $K_s = 1$ [13]. The LL Hamiltonian completely decouples when expressed in terms of spin and charge boson fields [13], and the Zeeman term H_Z affects only the spin sector. Written in terms of right- and left-moving fermions $\psi_{R/L}$, the continuum version of Eq. (3) is (up to irrelevant terms) $H' = H_1 + H_2$ with

$$H_1 = \int dx\, \vec{\lambda} \cdot (\vec{J}_L - \vec{J}_R)\,, \quad (5)$$

$$H_2 = \int dx \sum_{r=R/L} \psi_r^\dagger \vec{\lambda}' \cdot \vec{\sigma} i \partial_x \psi_r + \text{H.c.} \quad (6)$$

With the unit vector $\hat{e}_t$ along the tube axis, we use

$$\vec{\lambda} = 2\,\text{Im} \sum_a e^{i\vec{K}\cdot\vec{\delta}_a} \vec{u}_a, \qquad \vec{\lambda}' = \sum_a e^{i\vec{K}\cdot\vec{\delta}_a} (\hat{e}_t \cdot \vec{\delta}_a) \vec{u}_a\,,$$

and neglect oscillatory terms which average out on large length scales. These oscillations are governed by the wave vector $2k_F$ corresponding to the doping level μ, $k_F = |\mu|/v_F$, with typical values $|\mu| \approx 0.3$ to 0.5 eV [14]. Finally, $\vec{J}_{R,L} = \psi_{R/L}^\dagger (\vec{\sigma}/2) \psi_{R/L}$ are the standard SU(2) spin currents. The perturbation (5) has scaling dimension 1 (relevant), whereas Eq. (6) has dimension 2 (marginal). Therefore the leading SO contribution retained in what follows is Eq. (5).

Remarkably, the SO interaction (5) acts exclusively in the spin sector and hence does *not spoil spin-charge separation*. As a consequence, since electron-electron interactions affect only the charge sector, the ESR intensity can be computed using the equivalent fermionic spin Hamiltonian

$$H_f = \sum_{r=R/L=\pm} \int dx\, [-ir v_s \psi_r^\dagger \partial_x \psi_r + \vec{\lambda}_r \cdot \vec{J}_r], \quad (7)$$

where $\vec{\lambda}_\pm = \vec{B} \pm \vec{\lambda}$. Since H_f is bilinear in the fermions, after some straightforward algebra, the exact ESR spectrum follows for arbitrary temperature

$$I(\omega) = \sum_{r=\pm} \left(1 + \frac{\lambda_r^z}{\lambda_r}\right)^2 \frac{\lambda_r}{4v_s(1 - e^{-\lambda_r/T})}\, \delta(\omega - \lambda_r)\,, \quad (8)$$

with $\lambda_\pm = |\vec{\lambda}_\pm|$. As a consequence of SO coupling, the single δ peak *splits into two peaks* but there is no broadening. The peak separation is $|\lambda_+ - \lambda_-|$, and the peak

heights are generally different. To lowest order in λ/B, the two peaks are located symmetrically around $\omega = B$. Notice that, for $\vec{B}$ perpendicular to the effective SO vector $\vec{\lambda}$, the splitting is zero. It should be stressed that these results hold both for the noninteracting and the interacting case. The double peak is therefore not directly related to the doubling of singularities in the single-electron Greens function commonly associated with spin-charge separation. However, for the interacting case realized in SWNTs [3], the double peak structure is only possible if spin-charge separation is present. Otherwise the charge sector will mix in, leading to broad bands with threshold behaviors [8]. Closer inspection shows that inclusion of the subleading term (6) preserves the splitting into two peaks, but the peaks now acquire a finite width $\sim|\vec{\lambda}'|$.

Experimental observation of the predicted double peak spectrum could then provide strong evidence for spin-charge separation. In practice, to get measurable intensities, one will have to work with an ensemble of SWNTs. The proposed experiment may be possible using electric-field-aligned SWNTs, or by employing arrays of identical SWNTS [15]. In more conventional samples containing many SWNTs, however, the SO vector $\vec{\lambda}$ can take any direction. Assuming a uniform probability distribution for the orientation of $\vec{\lambda}$, the average can easily be done. For $T = 0$ and $\vec{\lambda}' = 0$, we find

$$\overline{I(\omega)} = \frac{[(\omega + B)^2 - \lambda^2]^2}{16 v_s B^3 \lambda}\,\theta(B + \lambda - \omega) \times \theta(\omega - |B - \lambda|)\,, \tag{9}$$

with the Heaviside function $\theta(z)$. For $B > \lambda$, this asymmetric spectrum has the width $\Delta\omega = 2\lambda$, which in turn allows us to extract the SO coupling strength λ from ESR measurements.

For the remainder, we then focus on MWNTs where we first contemplate a simple two-shell model. Experimental evidence [4] is consistent with the assumption that intershell tunneling is strongly suppressed. Therefore doping due to charge transfer from the substrate, the attached leads, or due to oxygen absorption, should affect only the outermost shell, while $\mu \approx 0$ for inner shells. Under this assumption, basically all conduction electrons contributing to the ESR signal reside in the outermost shell. Moreover, the electrostatic potential Φ_o of the outer shell differs from the inner-shell potential Φ_i. In effect, we can then restrict attention to the outermost shell (of radius R) alone, but in a radial electric field of size $E \approx 2c_{12}\Delta\Phi/R$, where c_{12} is the intershell capacitance per length and $\Delta\Phi = \Phi_i - \Phi_o$. The general expression (4) for the SO vector then yields after some algebra for a given bond $\vec{\delta}_a$,

$$\vec{u}_a = (u/v_F)\hat{E} \times \vec{\delta}_a\,, \tag{10}$$

where $\hat{E}$ is a unit vector perpendicular to the tube surface, and $u \approx c_{12} e \Delta\Phi/(m^2 d R)$ with the C-C distance $d = 1.42$ Å.

To proceed, we turn to the low-energy theory, again for only one K point. The influence of interactions is expected to be less dramatic in MWNTs compared to SWNTs, and here we focus on the noninteracting case. In real space, we then have a Dirac Hamiltonian, $H_0 = -i v_F \int d\vec{r}\, \Psi^\dagger(\vec{\tau}\cdot\vec{\nabla})\Psi$, where the integral extends over the tube surface and the Pauli matrices $\vec{\tau}$ act in sublattice space. The SO contribution appropriate for MWNTs follows by inserting Eq. (10) into Eq. (3), which yields the manifestly Hermitian term

$$H' = -iuv_F \int d\vec{r}\, \Psi^\dagger(\tau^-\sigma^+ - \tau^+\sigma^-)\Psi\,. \tag{11}$$

We take the magnetic field parallel to the tube axis and include both orbital and Zeeman contributions [16].

The full Hamiltonian can then be diagonalized. The dispersion relation contains four branches, $\epsilon(\vec{k}) = \pm\epsilon_\pm(k)$, where the $\pm$ signs are independent and

$$\epsilon_\pm(k) = [v_F^2(k^2 + Q^2) + (B/2)^2 \pm v_F\{(B^2 + 2v_F^2 Q^2)k^2 + v_F^2 Q^4\}^{1/2}]^{1/2}, \tag{12}$$

with $Q = 2\sqrt{2}\,u$ measuring the SO strength and $k = |\vec{k}|$. Using Eq. (12), the ESR intensity at finite temperature T reads

$$I(\omega) = \frac{-1}{1 - e^{-\omega/T}} \int \frac{d\vec{k}}{8\pi} \frac{\Pi(\epsilon_+, k; \omega)\delta(\omega - \epsilon_+ + \epsilon_-)}{\epsilon_+\epsilon_-(\epsilon_+^2 - \epsilon_-^2)^2} \times [n_F(\epsilon_+) - n_F(-\epsilon_+) - n_F(\epsilon_-) + n_F(-\epsilon_-)], \tag{13}$$

where $n_F(\epsilon) = 1/(1 + e^{-(\mu-\epsilon)/T})$ is the Fermi-Dirac distribution function. The integral in Eq. (13) includes an integration over the momentum parallel to the MWNT axis and a discrete summation over the quantized transverse momenta, $k_\perp = (n - \phi)/R$, where $\phi = \pi R^2 B/(h/e)$ is due to the orbital effect of the applied magnetic field and the summation extends over integer n. Furthermore, with $\bar{\omega}' = \omega' - \omega$ and $f(\omega', k) = v_F^2 k^2 - (B/2 + \omega')^2$,

$$\Pi(\omega', k; \omega) = 2f(\omega', k)f(-\bar{\omega}', k)[(B/2 - \omega')(B/2 + \bar{\omega}') - v_F^2 k^2] - 2v_F^2 Q^2[(B/2 - \omega')(B/2 - \bar{\omega}')f(\omega', k) + (B/2 + \omega')(B/2 + \bar{\omega}')f(-\bar{\omega}', k)]. \tag{14}$$

As a simple check, for $Q = 0$, one recovers the expected δ peak from Eq. (13).

The result (13) can be understood in simple physical terms. The ESR intensity receives contributions from transitions between states of energy ϵ_- to states of energy ϵ_+, and each contribution is weighted by a factor which takes into account the occupation of the levels. In order to arrive at Eq. (13), we have neglected a contribution coming from transitions between $-\epsilon_\pm$ and $\epsilon_\mp$ states. This is consistent

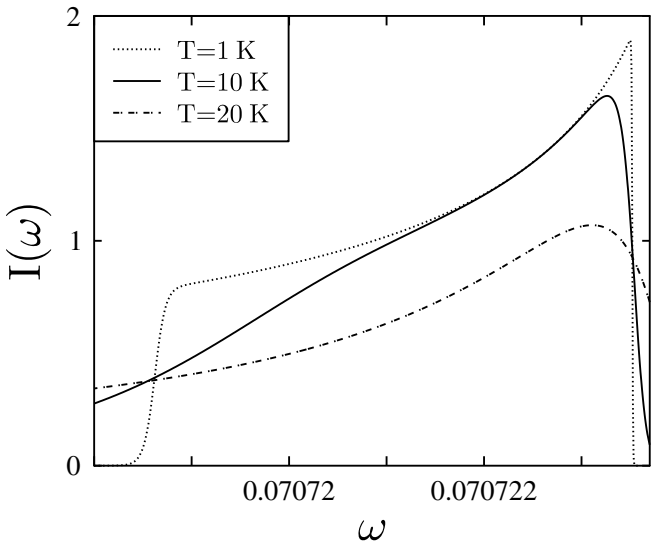

FIG. 1. Typical ESR intensity of a MWNT at low temperatures. Parameters in the plot are $\phi = 0$, $\mu = 0.1$, $B = 0.0014$, and $v_F Q = 0.05$, where energies are measured in units of $2\pi\hbar v_F/R$. The value of B corresponds to a field of 10 T. Note the frequency units, pointing to a very narrow ESR peak.

because these transitions contribute only for very large frequencies $\omega \geq |\mu|$, while the frequency scales relevant to ESR are much lower. In addition, the signal given by this contribution is very small in comparison to the term that we keep.

Inspection of Eq. (13) shows that the ESR spectrum of a MWNT at low temperatures contains only a *single narrow asymmetric peak,* whereas more structure appears at higher temperature due to the activation of the transverse subbands [17]. Here we focus on the low-temperature ESR spectrum, which is shown in Fig. 1 for typical parameters. The peak has an asymmetric line shape which strongly depends on temperature. At zero temperature, the intensity maximum is at the frequency

$$\omega_0 = \epsilon_Z \left[1 - \frac{\epsilon_Z^2}{2\mu^2} - \frac{v_F^2 Q^2 B^2}{4\mu^2 \epsilon_Z^2} + \mathcal{O}[(\epsilon_Z/\mu)^3] \right], \tag{15}$$

where $\epsilon_Z = \sqrt{B^2 + 2v_F^2 Q^2}$. As is apparent in Fig. 1, when increasing the temperature, the position of the maximum slowly moves to smaller frequencies. The linewidth is of the order of

$$\Delta\omega \approx v_F^2 Q^2 B^2/\mu^3. \tag{16}$$

To conclude, we have presented a theoretical description of the spin-orbit coupling and the ESR spectrum for 1D conductors, in particular for carbon nanotubes. In SWNTs, spin-charge separation should not be affected by spin-orbit coupling, and hence we expect a double peak. The peaks distance and their height provide information about the spin-orbit coupling strength, and their width points to violations of spin-charge separation. The ESR spectrum of a MWNT exhibits only a single narrow peak, whose location, line shape, and linewidth provide information about the Rashba-type spin-orbit coupling and intrinsic electric fields. The ESR spectra of SWNTs and MWNTs are therefore fundamentally different and reflect distinct mechanisms of spin-orbit coupling.

We thank L. Forró for discussions. Support by the DFG under the Gerhard-Hess program and by the project PICT 99 3-6343 is acknowledged.

[1] M. Oshikawa and I. Affleck, Phys. Rev. Lett. **82**, 5136 (1999); cond-mat/0108424.
[2] C. Dekker, Phys. Today **52**, No. 5, 22 (1999); see also reviews on nanotubes in special issue of Phys. World **6** (2000).
[3] M. Bockrath *et al.,* Nature (London) **397**, 598 (1999); Z. Yao *et al., ibid.* **402**, 273 (1999); H. Postma *et al.,* Science **293**, 76 (2001).
[4] L. Forró and C. Schönenberger, in *Carbon Nanotubes,* edited by M. S. Dresselhaus *et al.,* Topics in Applied Physics Vol. 80 (Springer, New York, 2001).
[5] R. Egger and A. O. Gogolin, Phys. Rev. Lett. **79**, 5082 (1997); C. Kane, L. Balents, and M. P. A. Fisher, *ibid.* **79**, 5086 (1997).
[6] L. Balents and R. Egger, Phys. Rev. Lett. **85**, 3464 (2000); Phys. Rev. B **64**, 035310 (2001).
[7] A. V. Moroz, K. V. Samokhin, and C. H. W. Barnes, Phys. Rev. Lett. **84**, 4164 (2000); see, however, W. Häusler, Phys. Rev. B **63**, 121310 (2001); M. Governale and U. Zülicke, cond-mat/0201164.
[8] A. De Martino and R. Egger, Europhys. Lett. **56**, 570 (2001).
[9] We often put $\hbar = c = k_B = g_e \mu_B = 1$.
[10] G. H. Chen and M. E. Raikh, Phys. Rev. B **60**, 4826 (1999).
[11] N. E. Bonesteel, Phys. Rev. B **47**, 11 302 (1993).
[12] T. Ando, J. Phys. Soc. Jpn. **69**, 1757 (2000).
[13] A. O. Gogolin, A. A. Nersesyan, and A. M. Tsvelik, *Bosonization and Strongly Correlated Electron Systems* (Cambridge University Press, Cambridge, 1998).
[14] S. Lemay *et al.,* Nature (London) **412**, 617 (2001).
[15] R. R. Schlittler *et al.,* Science **292**, 1136 (2001).
[16] For SWNTs, the orbital term can always be neglected.
[17] A. De Martino, R. Egger, K. Hallberg, and C. A. Balseiro (to be published).